Sweeping vacuum gravitational waves under the rug

Negro, A.

CHAPTER 1

Introduction

All quantities that can be extracted by experimental measurements and/or observations are called *observables*. Observables, are measured at some fixed temporal and spatial location and involve either direct or indirect exchange of energy or momentum among propagating degrees of freedom and a detector. Unfortunately, however, it is not always the case that we can compute what we directly observe. What we can actually compute, instead, are *correlation functions*; weighted averages of correlations of certain quantities in space and time. Thankfully, certain observables can be expressed as the coincidence limit of correlation functions – the limit at which correlations are evaluated at the same spacetime point – and/or their derivatives. That said, in the coincidence limit of quantum field theory (QFT), correlation functions contain by construction [217], ultra-violet (UV) divergent contributions. In order to obtain well-defined coincidence limits, and by extension physical correlation functions that can be translated observation, UV divergences must be consistently reabsorbed through the renormalization procedure.

One of the most important correlation functions in physics, and especially in cosmology, is the *energy density*. The energy density describes "how much energy" there is at each point in spacetime, due to the matter fields living in it. One of the most interesting contributions to the energy density content of the primordial universe, is that of gravitational waves (GWs). Indeed, primordial GWs offer the possibility of constraining epochs that are not accessible with electromagnetic signals and, considering the recent successful developments on GWs detection, the possibility of opening this new window on the early universe is becoming more and more realistic. Although there are numerous mechanisms that can produce them, in this thesis we focus on GWs produced by the *vacuum*; they are the tensorial counterpart of primordial scalar quantum fluctuations that seeded galaxies. The reason behind this choice is that, importantly, their *renormalized* energy density, is connected to an observable, i.e., the measured abundance of the first light elements produced in the radiation dominated phase of the universe. Consequently, this link presents us with a promising pathway to constrain vacuum GWs without the need for their direct detection.

However, as we already mentioned, in order exploit such connection, the correlation function of interest, $\rho_{\rm gw}$, must be well-defined, and therefore renormalized. In contrast, and as we shall delineate in more detail in chapters that follow, the

current state of the art for the energy density of vacuum GWs

$$\rho_{\rm gw} \simeq \frac{A_t}{32\pi G_N}\left(\frac{k_{\rm UV}}{k_*}\right)^{n_t}\frac{1}{2n_t}\frac{1}{(a\tau)^2}, \tag{1.1}$$

is not the "finished product"; a well-defined quantity we can connect to observables. Although the energy density in 1.1 may not appear to be divergent, the infinities have been swept under the the rug of an arbitrary *UV cutoff*. And even though $k_{\rm UV}$ can in fact appear in intermediate steps of the renormalization procedure (e.g., during regularization), physically observable, i.e., fully renormalized, quantities *do not* depend on such cutoffs.

In this thesis, by carefully renormalizing the divergences arising in computing $\rho_{\rm gw}$, we not only obtain a finite, regulator-independent result, but we also qualitatively change the interpretation of current constraints on vacuum GWs. Our analysis reveals that vacuum GWs, by their very nature, only serve to renormalize background quantities and do not enter as an additional effective radiation-like species. We stress that a fundamental role in reaching this conclusion is played by properly following trough the renormalization procedure, which is not a way to *sweep divergences under the rug* by introducing a hard cutoff in divergent integrals. As we will see in what follows, it is instead a well-defined recipe to absorb UV-divergent contributions and extract meaningful physical predictions.

1.1 Big Bang cosmology

This section is intended as a non-technical introduction to motivate the study of vacuum quantum tensor fluctuations, which is the main focus of this thesis. We start by presenting the chronology of the evolution of the universe to contextualize our work, we then review the foundations of the standard cosmological model and we motivate why we expect the presence of vacuum quantum fluctuations in the early stages of our universe.

1.1.1 Thermal history

The Big Bang theory describes the evolution of the universe as the cooling and expansion of the initial plasma. In its very early stages the universe was a highly dense and hot plasma made of relativistic particles forming a thermal bath. Before entering into the details of the formalism used to describe the cosmological model, we review the thermal history of the universe following Kolb and Turner in [134], focusing on the earliest stages up to the dark age.

- **Plank epoch** (Time t corresponding to $t < 10^{43}$ s, temperature T corresponding to T$> 10^{32}$ K / T$> 10^{19}$ GeV): in the Plank epoch, referring to the first instants of cosmic time, currently established laws of physics may not have applied and the evolution of the plasma is assumed to be dominated by quantum effects of gravity.

- **GUT** ($t < 10^{36}$ s, T> 10^{29} K / T> 10^{16} GeV): during this earliest period a number of spontaneous symmetry breaking (SSB) phase transitions take place, which imply that the full symmetry of the theory is broken to a lower symmetry. The first SSB corresponds to the grand unification phase transition (GUT) after which the three forces of the Standard Model are not unified anymore.

- **Inflation** ($t < 10^{32}$ s, T> 10^{22} K / T> 10^{9} GeV): the universe is then expected to go through an inflationary phase during which it expands by a factor of the order of 10^{26}. As a consequence, the universe is supercooled, a second SSB occurs and strong interactions become distinct from electroweak interactions.

- **Electroweak epoch** ($t < 10^{12}$ s, T> 10^{15} K / T> 150 GeV) and **Quark epoch** ($t < 10^{5}$ s, T> 10^{12} K / T> 150 MeV): elementary particles acquire mass via the Higgs mechanism and strongly interacting particles are present in the universe as color-singlet-quark-triplet states (baryons) and color-singlet-quark- antiquark states (mesons).

- **Hadron epoch** ($t < 1$ s, T> 10^{10} K / T> 1 MeV): quarks are bound into hadrons and a fraction of baryons survive from the baryon-antibaryon annihilation due to a slight matter-antimatter asymmetry ([214, 135]). As the universe's temperature cool down various particles decouple from the thermal bath.

- **Neutrino** (ν) **decoupling** ($t \approx 1$ s, T$\approx 10^{10}$ K/ T$\approx$ 1 MeV): neutrinos decouple from the cosmic thermal bath and the neutron (n) to proton (p) ratio freezes.

- **Big Bang Nucleosynthesis** (BBN) ($t \approx 10^{3}$ s, T$\approx 10^{7}$ K / T$\approx$ 1 keV): protons and neutrons are bound into primordial atomic nuclei such as Hydrogen, Helium and Lithium so that the first light elements are formed. The primordial abundance predictions, which are in agreement with current experimental evidence ([78]), are one of the two main successes of the Big Bang theory.

- **Lepton epoch** ($t < 10$ s, T> 10^{9} K / T> 100 keV) to **photon** (γ) **epoch** ($t < 370 \cdot 10^{3}$ years, T> 4000 K / T> 0.4 eV): during the lepton epoch the universe is hot enough to keep leptons and anti-leptons in thermal equilibrium but, as the temperature drops below the mass of the electron, high-energy photons can no longer produce electron-positron ($e^{-/+}$) pairs.

- **Recombination** ($18 \cdot 10^{3}$ years $< t < 370 \cdot 10^{3}$ years, T$\approx$ 4000 K / T$\approx$ 0.4 keV): light nuclei and electrons become bound to form neutral atoms. The interactions keeping photons in thermal equilibrium with the primordial plasma becomes less and less effective and the universe becomes more and more transparent.

- **Cosmic Microwave Background** (CMB) ($t \approx 370 \cdot 10^{3}$ years, T$\approx$ 4000 K / T$\approx$ 0.4 eV): when photons are no longer in thermal equilibrium with

matter, they travel freely through space and the CMB radiation is emitted. Its experimental detection by Penzias and Wilson [181] is the second main success of the Big Bang theory.

- **Dark ages** ($t < 10^9$ years, T> 60 K): after photons decoupled from the primordial plasma, the dark age begins.

Later on, the large scale structure (LSS) of the universe began to form, followed by galaxies, culminating in the structure of the universe as it is today. The work presented in this thesis investigates the early stages of the evolution of the universe, from the initial moments of the inflationary phase to the Cosmic Microwave Background (CMB). As illustrated in Fig. 1.1, which represents the evolution of the universe, this period is just a small fraction of the Big Bang expansion. However, as we try to show in the following sections, it is enormously rich and fascinating.

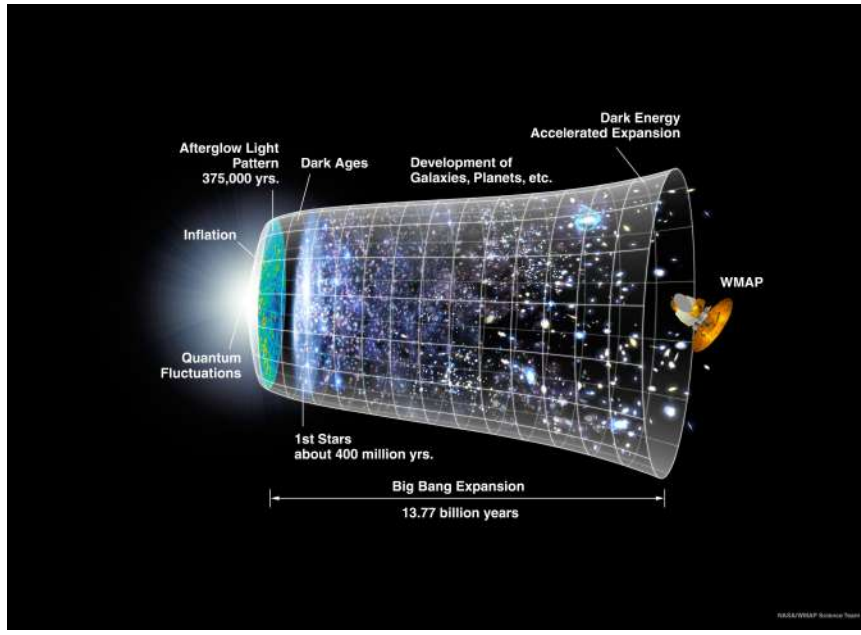

Figure 1.1: Representation of the evolution of the universe

The picture is a schematic representation of the Big Bang theory over 13.77 billion years, from left to right, inflationary evolution of the universe characterized by accelerated expansion, radiation/matter equality and dark ages.
Credit: NASA / WMAP Science Team.

1.1.2 Standard cosmological model

In this section, we aim to present the most important concepts of the standard cosmological model following the reviews by [88, 163].

The standard cosmological model is based on the cosmological principle, which can be stated as: *on sufficiently large scales the universe appears the same for all observers*, or, quoting Liddle [141]: *"the cosmological principle [means that] the universe looks the same whoever and wherever you are"*. Cosmological observations at sufficiently large scales (> 100 Mpc) validate the statement *the universe looks the same wherever you are* and, assuming that we are not special observers, validate the statement *the universe looks the same whoever you are*. This apparently simple statement implies that, at sufficiently large scales, our universe can be assumed homogeneous and isotropic. Requiring a homogeneous and isotropic solution for the Einstein equations (working in natural units in which $c = \hbar = 1$)

$$R_{\mu\nu} - \frac{1}{2} g_{\mu\nu} R = 8\pi G_N T_{\mu\nu}, \tag{1.2}$$

where $g_{\mu\nu}$ is the metric, $R_{\mu\nu}$ and R are the Ricci tensor and Ricci scalar respectively, G_N is the Newtonian constant and $T_{\mu\nu}$ is the stress energy tensor that we will better define in what follows, results in the so-called Friedmann-Lemaitre-Robertson-Walker (FLRW) metric ([103, 139, 187, 212])

$$ds^2 = g_{\mu\nu} dx^\mu dx^\nu = -dt^2 + a^2(t) \gamma_{ij} dx^i dx^j. \tag{1.3}$$

In the result for the FLRW metric in Eq. 1.3, $a(t)$ is the scale factor which encodes the time evolution of the universe and, as a result of the cosmological principle, it is a function of the cosmic time t only, x^μ are the comoving coordinates which are coordinates that move along with the overall expansion of the universe and γ_{ij} is the tensor corresponding to the spatial metric which, in spherical coordinates results[1]

$$\gamma_{ij} dx^i dx^j = \frac{dr^2}{1 - \kappa r^2} + r^2 d\phi^2 + r^2 \sin\theta^2 d\theta^2 \tag{1.4}$$

where κ is the intrinsic curvature of the spatial surfaces and, modulo a rescaling the coordinates, represents flat ($\kappa = 0$), negatively curved ($\kappa = -1$) or positively curved ($\kappa = 1$) spatial slices.

To describe the dynamic of the universe, one only has to solve Eq. 1.2 for the scale factor and, to do so, it is necessary to specify the stress energy tensor $T_{\mu\nu}$ of the field sourcing the universe. To be consistent with the symmetries of the metric, $T_{\mu\nu}$ must be diagonal and the spatial components must be equal. The simplest realization of such requirements is to assume that the universe is sourced by a perfect fluid characterized by a stress energy tensor of the form

$$T_{\mu\nu} = (\rho + p) u_\mu u_\nu + p g_{\mu\nu} \tag{1.5}$$

where ρ is the energy density, p the pressure and u_μ is the four velocity (which is $u^\mu = (1, 0, 0, 0)$ in a comoving coordinate system). If the fluid is assumed to be

[1] Greek indices take the value $(0, 1, 2, 3)$ and Latin indices take the value $(1, 2, 3)$.

barotropic, we can express the pressure in terms of the energy density trough the equation of state

$$p = p(\rho). \tag{1.6}$$

In the standard cosmological model the equation of state is a linear relation of the form

$$p = w\rho \tag{1.7}$$

where w is a dimensionless parameter. Considering the the conservation laws associated with the energy-momentum tensor

$$\nabla_\mu T^{\mu\nu} = 0, \tag{1.8}$$

we obtain that the spatial components are trivially satisfied while the zero-component results in the continuity equation

$$\dot{\rho} = -3H(\rho + p) \tag{1.9}$$

where we define $\dot{\rho} := \frac{d\rho}{dt}$ and the Hubble parameter $H(t) := \frac{\dot{a}}{a}$. Considering Eq. 1.7, the continuity equation results

$$\rho a^{3(1+w)} = \text{constant} \tag{1.10}$$

and, specifying the value of w we obtain

$$\begin{aligned} \text{MATTER}: &\qquad w = 0 \;\Rightarrow\; \rho_m a^3 = \text{constant} \\ \text{RADIATION}: &\qquad w = \frac{1}{3} \;\Rightarrow\; \rho_r a^4 = \text{constant} \\ \text{COSMOLOGICAL CONST}: &\qquad w = -1 \;\Rightarrow\; \rho_\Lambda = \text{constant}. \end{aligned} \tag{1.11}$$

In the standard ΛCDM model one assumes that the universe is mostly dominated by the so-called dark energy Λ, corresponding to $w = -1$, and cold dark matter, corresponding to $w = 0$. Before that, the early universe is assumed to be mostly composed by radiation (the so-called radiation dominated (RD) era) which follows a primordial vacuum-dominated era (inflation). By using the results of Eq. 1.11, we can express ρ and p in terms of the scale factor and straightforwardly solve the Einstein equations in Eq. 1.2.
The (00) component and any of the non-zero (ij) components of Eq. 1.2 result[2]

$$\begin{aligned} -3\frac{\ddot{a}}{a} &= 4\pi G_N(\rho + 3P) \\ \frac{\ddot{a}}{a} + 2\frac{\dot{a}^2}{a^2} + 2\frac{\kappa}{a^2} &= 4\pi G_N(\rho - P) \end{aligned} \tag{1.12}$$

and, by combining the two equations, we obtain the so-called Friedmann equations [102]

$$\begin{aligned} H^2 &= \frac{\rho}{3M_{\rm pl}^2} - \frac{\kappa}{a^2} \\ \dot{H} + H^2 &= -\frac{1}{6M_P^2}(\rho + 3p), \end{aligned} \tag{1.13}$$

[2] As a consequence of isotropy there are only two independent equations by specifying Eq. 1.2 in components.

where we define the reduced Planck mass as $M_{\rm pl} = \sqrt{\frac{1}{8\pi G_N}}$. Combining Eqs. 1.13 with the continuity equation[3] in Eq. 1.9 we can solve for the scale factor. By defining the critical density $\rho_{\rm c}$ and the parameter Ω as

$$\rho_{\rm c} := 3M_{\rm pl}^2 H_0, \quad \Omega_i := \frac{\rho_i}{\rho_{\rm c}}, \tag{1.14}$$

where we denote as H_0 the Hubble parameter at present time, we can re-write the first Friedmann equation as

$$H^2 = H_0^2 \left[\Omega_r \left(\frac{1}{a}\right)^4 + \Omega_m \left(\frac{1}{a}\right)^3 - \frac{\kappa}{H_0^2}\left(\frac{1}{a}\right)^2 + \Omega_\Lambda \right]. \tag{1.15}$$

We then consider that by CMB observations the universe appears to be flat (i.e., we assume $\kappa = 0$, [7]) to integrate Eq. 1.15 and obtain the scale factor as a function of the cosmic time t. We obtain that in the case of a RD, matter dominated and Λ-dominated universe, the scale factor results respectively

$$\dot{a} \sim a^{\frac{1}{2}(1+3w)} \Rightarrow a(t) = \begin{cases} t^{\frac{1}{2}} & \text{RADIATION} \quad (w = \frac{1}{3}) \\ t^{\frac{2}{3}} & \text{MATTER} \quad (w = 0) \\ e^{Ht} & \text{COSMOLOGICAL CONST} \quad (w = -1). \end{cases} \tag{1.16}$$

For convenience, we define the conformal time τ trough the following relation $d\tau = \frac{dt}{a}$. In conformal coordinates, the FLRW metric in Eq. 1.3 can be rewritten as

$$ds^2 = a^2(\tau)(-d\tau^2 + \gamma_{ij} dx^i dx^j) = a^2(\tau)(-d\tau^2 + \delta_{ij} dx^i dx^j), \tag{1.17}$$

where in the second equality we assume $\kappa = 0$ to highlight that τ is called conformal time as the FLRW line element results conformal to the Minkowski line element, describing a static 4-dimensional hypersurface.
As in what follow we mostly use the conformal time, we recall that the relation between the Hubble parameter in cosmic time and conformal time results $H = \frac{\mathcal{H}}{a}$ and the first Friedmann equation and the continuity equation result respectively

$$\begin{aligned} \mathcal{H}^2 &= \frac{\rho a^2}{3M_{\rm pl}^2} - \kappa \\ \rho' &= -3\mathcal{H}(\rho + p), \end{aligned} \tag{1.18}$$

where we denote the derivative with respect to conformal time as $a' := \frac{da(\tau)}{d\tau}$ and the Hubble parameter in conformal time as $\mathcal{H} = \frac{a'}{a}$. Therefore, repeating the previous steps we find that in the RD era the scale factor results $a(\tau) \sim \tau$ and in the matter dominated era the scale factor results $a(\tau) \sim \tau^2$.

[3] Note that the continuity equation can be also derived by combining Friedmann equations, as a consequence of the Bianchi identities.

This apparently simple description allows us to explore many early universe phenomena with a single parameter: $a(t)$. Furthermore, as we derived how the scale factor evolves depending on the content of the universe, by knowing the values of the density parameters today (Ω_m, Ω_r and Ω_Λ), we can infer the expansion of the universe throughout its evolution. On one hand, the description reviewed in this section is successfully confirmed by the experimental evidences of CMB radiation. On the other hand, CMB brings to light some of the biggest puzzles of the modern cosmology (see [127, 144, 118, 75, 180, 175] for some examples). Assuming that the universe is homogeneous and isotropic would not account for the the formation of the structures that we see nowadays in the universe, such as galaxies, stars and planets. In the next section we review the so-called "primordial seeds": vacuum quantum perturbations.

1.1.3 Perturbation theory and vacuum perturbations

From CMB observations, as shown in Fig. 1.2, it is evident that the early universe was very nearly uniform. However, it is thanks to the word 'nearly' that we can explain our existence.

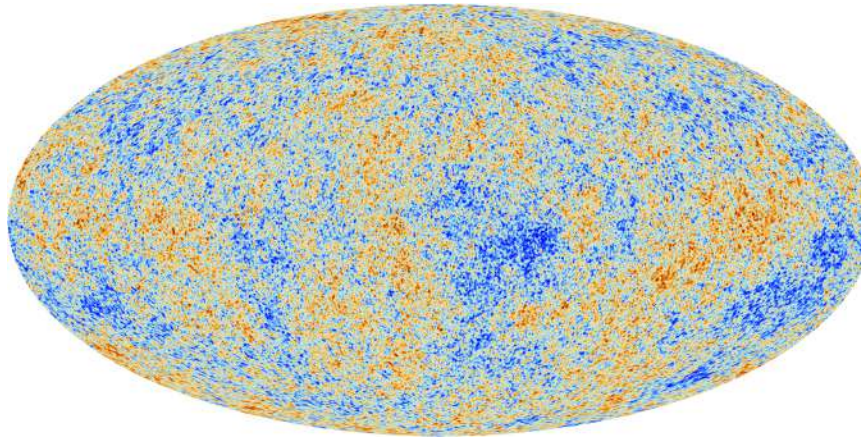

Figure 1.2: Cosmic Microwave Background

The CMB is the first picture of our universe that can be detected. The early universe (just 380,000 years old) appears surprisingly homogeneous and isotropic. Temperature fluctuations of the order of 10^{-5} are the the observational confirmation of the "primordial seeds".
Credit: ESA, Planck Collaboration.

The presence of vacuum quantum fluctuations, which are primordial departures from the homogeneous and isotropic configuration, is our current understanding of LSS formation of the universe. Such small perturbations can be treated in the context of perturbation theory up to the matter dominated era when, thanks to gravitational instabilities, some seeds grew to originate the structures that we ob-

serve ([179]). In what follows we review the so-called cosmological perturbation theory following [132, 153].

We consider a perturbation $h_{\mu\nu}$ around the FLRW solution

$$g_{\mu\nu} = g_{\mu\nu}^{\text{FLRW}} + h_{\mu\nu} \tag{1.19}$$

which, in conformal time can be rewritten as

$$g_{\mu\nu} = a^2\eta_{\mu\nu} + h_{\mu\nu}, \tag{1.20}$$

where $\eta_{\mu\nu}$ is the Minkowski metric. As the FLRW background is under spatial rotations, one can break down the metric perturbation $h_{\mu\nu}$ into irreducible representations of Euclidian rotations[4]. This is the so-called scalar vector tensor (SVT) decomposition, first introduced by Lifshitz [143]. As a consequence, the perturbed line element can be written as

$$ds^2 = a^2\left[-(1+2\psi)d\tau^2 + 2w_i d\tau dx^i + (1+2\phi)\delta_{ij}dx^i dx^j + 2S_{ij}dx^i dx^j\right], \tag{1.21}$$

where ψ and ϕ are two scalar gravitational potentials, w_i is a vector and S_{ij} is traceless under the spatial part of the background metric.
Similarly to the metric, the stress energy tensor is decomposed as a background part $\bar{T}_{\mu\nu}$, which sources the background metric, and perturbation $\delta T_{\mu\nu}$. In this way, the components of the stress energy tensor result

$$\begin{aligned}
T_0^0 &= -\left(\bar{\rho} + \delta\rho\right), \\
T_i^0 &= \left(\bar{\rho} + \bar{p}\right)(v_i + w_i), \\
T_0^i &= \left(\bar{\rho} + \bar{p}\right)v^i i, \\
T_j^i &= \bar{p}\delta_j^i + \left(\delta p\delta_j^i + \Pi_j^i\right),
\end{aligned} \tag{1.22}$$

where background quantities $(\bar{\rho}, \bar{p})$ are functions of the time only, Π_j^i accounts for velocity gradients and v^i is the spatial perturbation of the peculiar velocity.
The last ingredient that one has to consider before tackling the study of cosmological perturbations is that, under an infinitesimal change of coordinates

$$x'^\mu = x^\mu + \xi^\mu, \tag{1.23}$$

the metric perturbation transforms as

$$h'_{\mu\nu} = h_{\mu\nu} - \bar{\nabla}_\mu\xi_\nu - \bar{\nabla}_\nu\xi_\mu \tag{1.24}$$

where $\bar{\nabla}_\nu$ is the covariant derivative built with the FLRW background metric. General relativity (GR) is invariant under change of coordinates, which implies that the change of coordinates in Eq. 1.23 does not effect observable results. As an important consequence, we obtain that the transformation in Eq. 1.24, called gauge

[4] In representation theory, this corresponds to decomposing perturbations under the group of spatial rotations.

transformation, does not have physical implications, it highlights a redundancy of our description and the need of fixing a gauge.
At this point, one can consider the perturbed line element in Eq. 1.21, the perturbed stress energy tensor in Eq. 1.22 and, being mindful of fixing the gauge, describe the evolution of primordial perturbations by deriving the perturbed Einstein equations in Eq. 1.2 (among the many references on perturbation theory and the observable consequences of including vacuum quantum perturbations, see [46, 153, 165, 32, 6, 192, 39, 5, 186, 19, 119, 105, 113] for some examples). In the next chapters we will review the details of this procedure, focusing our attention on tensor vacuum perturbations, or vacuum GWs.

1.2 Quantum corrections and infinities

What are quantum corrections? How do we quantify them? How do they correct the classical answer? The answers to these questions, that we now review, are the guideline of the work presented in this thesis.

We consider the cross section of the e^+/e^- scattering process[5] σ_e, which is a natural quantity to be measured experimentally. In the context of second quantization we can derive the Feynman diagrams contributing to the process at arbitrarily high order in $\hbar$. The diagrams of order $\hbar^0$, the so-called tree diagrams, represent the classical answer and graphs corresponding to higher orders in $\hbar$, loop diagrams, represent the quantum corrections to the classical answer (See Fig. 1.3 for examples of tree diagrams and the first order loop corrections).
Once we include loop diagrams in the estimate of σ_e, infinities arise in the short distance limit, which take the name of UV divergences. Infinities often arise when computing physical observables in any quantum or statistical field theoretic framework, and this naturally rise the question of how to deal with such apparently meaningless results. As a consequence, the renormalization procedure has been developed so that quantum corrections can be consistently included in the estimate of observables.
Following trough the renormalization procedure, one realizes that the diagrammatic splitting into tree diagrams and loop diagrams can be misleading as calculations of quantum corrections tell us nothing of loops absolute values. Even if certain properties of observables can be explained as coming uniquely from quantum effects[6], in measuring the scattering amplitude σ_e one cannot separately measure the tree level and loop corrections and, in general, all physical observations are necessarily of fully dressed quantities; as a result, the tree diagram around which one computes the quantum corrections is only to be viewed as a calculational fiction that serves as bootstrap into computing physical observables.

[5] the electron positron scattering takes the name of Bhabha scattering ([47]).
[6] It is the case of the Casimir effect ([69, 137]), anomalies ([11, 159]) or running of coupling constants ([116, 117]).

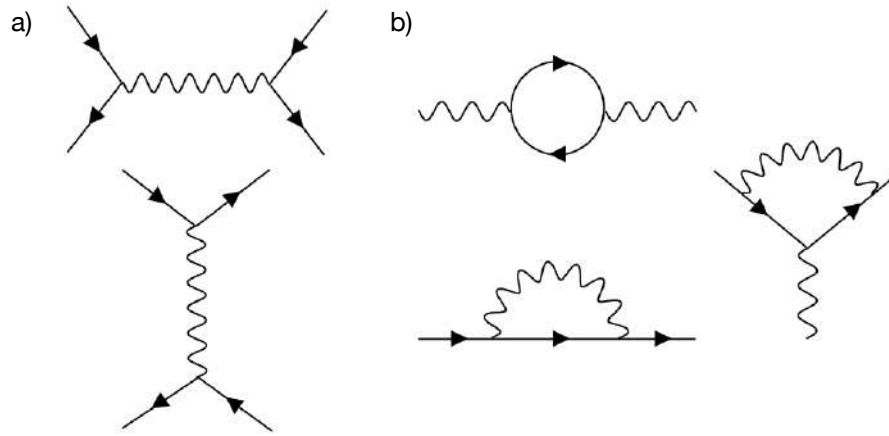

Figure 1.3: Examples tree and 1-loop Feynman diagrams in QED.

a) Examples of tree level QED Feynman diagrams in QED (s-channel and t-channel of Bhabha scattering). **b)** 1-loop QED Feynman diagrams.

1.2.1 UV and IR divergences

Before reviewing the details of the renormalization procedure and discuss the divergences arising in computing the vacuum energy, we comment on the differences between UV divergences and infra-red (IR) divergences.

Divergences can typically be categorized into two types, each with its own distinct physical meaning. On one hand, short distance or UV divergences are cured with the well-defined prescription of renormalization, which we review in the next section[7]. The regularization of UV divergences has been developed on flat backgrounds and, as we will discuss in this thesis, a transposition of this formalism to curved backgrounds is possible, albeit with numerous caveats and subtleties that one must be mindful of depending on the context [48, 178, 164]. UV divergences arise in including quantum corrections and are the result of the mathematical idealization of probing arbitrarily small scales by admitting arbitrarily high energies in any given calculation. Once these infinities have been appropriately subtracted, causality and locality prevent such idealization [205, 26] and operators can be classed by derivative expansion into relevant, marginal and irrelevant operators (see e.g. [130, 61, 155]).

On the other hand, long wavelength or IR divergences require additional care in their interpretation. At the very least, they indicate that one has additional

[7] Among the many references introducing this topic such as [125, 218, 215, 194], see the treatment of Kleinert in [130] in the context of renormalizable theories and of Burgess in [61] in the context of effective field theories.

work to do in order to arrive at a physical quantity. IR divergences can appear in intermediate expressions in theories with gapless excitations, and cancel out when computing physical observables. As an example, this is the case of soft photons in quantum electrodynamics (QED) ([49]) where, by considering that an arbitrarily large numbers of soft photons is not detected due to limited sensitivity of the experimental apparatus, one obtains an intermediate IR divergent result for certain scattering processes. However, such IR divergencies cancel when virtual soft photons are included and all the diagrams contributing to the process are summed.
IR divergences could also appear because of the breakdown of a particular perturbative scheme. This can be cured through resummation, as is the case when one studies thermalization in an out of equilibrium context [66, 45], or in quantum chromodynamics (QCD) scattering via the factorization properties of its soft and collinear limits [136, 148].
In the most problematic scenario, IR divergences arise as a consequence of the instability of the background around which one is attempting to perturb. This is particularly relevant for cosmology, as a class of IR divergences arise perturbing around de Sitter (dS) or quasi dS bacgkrounds ([101, 162, 25, 89, 20, 122, 62, 108, 174, 126, 183, 15, 16, 21, 114]) and one cannot rely on standard background field quantization methods. Large quantum corrections to the background could invalidate the split between classical background and fluctuations, which is a limiting case of the general complication of doing perturbation theory around a time evolving background that must satisfy the tadpole condition at any given order in $\hbar$. As a consequence, stochastic inflation and its background statistical field theory limit is used to tackle this problem ([202, 33, 185, 110, 168, 166, 167, 161, 189, 145, 203, 99, 95, 100, 182, 211, 29, 96, 23, 31, 209, 77]) as well as dynamical renormalization group and open effective field theory approaches [52, 64, 63].
However, as reviewed [35, 197], in situations where one can presume the validity of background field quantization, which is the assumption for this thesis, it is possible to extract meaningful results and well defined observables in spite of the appearence of IR divergences in inflationary cosmology.

In what follows we will put extra care in commenting the appearance of IR divergences; however, as we aim to focus on the study of UV divergences in early universe observables, in the next section we review the details of subtracting and renormalizing UV divergent quantities.

1.2.2 Renormalization

In this section we introduce the renormalization procedure by computing the QED vacuum polarization diagram (see [194, 218] for more details). We aim to review the recipe that leads to a finite, physical result and highlight the steps that one needs to follow in order to consistently reabsorb UV divergences arising from including quantum corrections.

We consider the Lagrangian of QED

$$\mathcal{L}_{\text{QED}} = \frac{1}{4} F_{\mu\nu} F^{\mu\nu} + i\bar{\psi}(\not{\partial} + ie\not{A})\psi - m\bar{\psi}\psi, \tag{1.25}$$

where $F^{\mu\nu}$ is the electromagnetic tensor that, as a function of the electromagnetic potential[8] A_μ, results $F_{\mu\nu} = \partial_\mu A_\nu - \partial_\nu A_\mu$, $\psi/\bar{\psi}$ is are fermionic fields that represent the electron/positron, m and e represent the mass and the charge of the electron. From the Lagrangian in Eq. 1.25 one can derive the Feynman rules that allow to straightforwardly obtain the following result

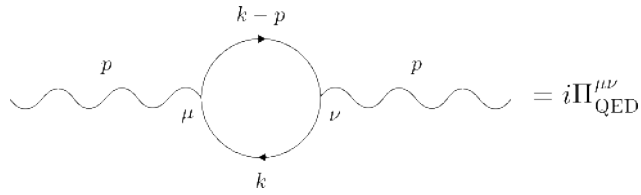

Figure 1.4: Self energy of photon

Feynman diagram representing the vacuum polarization loop diagram in QED.

$$i\Pi^{\mu\nu}_{\text{QED}} = -(-ie)^2 \int \frac{d^4k}{(2\pi)^4} \frac{(i)^2 \,\text{Tr}\,[\gamma^\mu(\not{k} - \not{p} + m)\gamma^\nu(\not{k} + m)]}{[(p^\alpha - k^\alpha)^2 - m^2 + i\epsilon][k^\alpha k_\alpha - m^2 + i\epsilon]}. \tag{1.26}$$

As a consequence, by computing the integral in Eq. 1.26 we can quantify the contribution of the loop diagram represented in the Feynman graph in Fig. 1.4. The trace of the gamma matrices results (See Appendix A of [194] for more details)

$$\text{Tr}\,[\gamma^\mu(\not{k} - \not{p} + m)\gamma^\nu(\not{k} + m)] = 4[-p^\mu k^\nu - k^\mu p^\nu + 2k^\mu k^\nu + \eta^{\mu\nu}(p^\alpha k_\alpha - k^\alpha k_\alpha + m^2)] \tag{1.27}$$

and, dropping the p^μ and p^ν terms as they do not contribute for symmetry reasons, we obtain

$$i\Pi^{\mu\nu}_{\text{QED}} = -4e^2 \int \frac{d^4k}{(2\pi)^4} \frac{2k^\mu k^\nu + \eta^{\mu\nu}(p^\alpha k_\alpha - k^\alpha k_\alpha + m^2)}{[(p^\alpha - k^\alpha)^2 - m^2 + i\epsilon][k^\alpha k_\alpha - m^2 + i\epsilon]}. \tag{1.28}$$

The loop contribution in Eq. 1.28 is unsurprisingly divergent in the $k \to \infty$ limit. In what follows, we review the procedure that allows to extract a physical meaning from divergences arising in including quantum corrections.

1) Explicit the appearance of the divergent structure (regularization)

The first step is to isolate the divergent structure of Eq. 1.28 with the help of a regulator. This procedure is called regularization and can be done in different ways,

[8] We use the Feynman slash notation, where slashed quantities are covariant quantities contracted with gamma matrices: $\not{A} = A_\mu \gamma^\mu$.

using different regularization methods. A regulator is a nonphysical parameter that one inserts to factor the divergent structure and, by definition, it cannot appear in the final result.

To introduce the regularization methods that will be used in this thesis, we review the regulators of dimensional regularization, hard cutoffs and Hadamard regularization. In the case of dimensional regularization, the dimension of the measure of the integral is generalized to $D = 4 - \delta$ dimensions, δ represents the regulator and divergences are written as poles in δ: $\lim_{\delta\to 0} \frac{1}{\delta}(...)$. In the case of hard cutoffs, the regulator can be a cutoff energy scale $\Lambda_{\rm UV}$ and divergences are written as functions that diverge in the limit $\Lambda_{\rm UV} \to \infty$. Lastly, in the case of Hadamard regularization, the regulator is the geodesic distance from two points σ^μ and divergences are rewritten as poles in the coincidence limit.
To dimensionally regularize Eq. 1.28, we use the Feynman parameter trick:

$$\frac{1}{AB} = \int_0^1 dx \frac{1}{[A + (B - A)x]^2} \tag{1.29}$$

and we shift the integration variable as $k^\mu \to k^\mu + p^\mu(1 - x)$, to obtain[9]

$$\Pi^{\mu\nu}_{\rm QED} = 4ie^2 \int \frac{d^4k}{(2\pi)^4} \int_0^1 dx \frac{2k^\mu k^\nu - \eta^{\mu\nu}(k^2 - p^2x(1 - x) - m^2)}{[k^2 + p^2x(1 - x) - m^2 + i\epsilon]^2}. \tag{1.30}$$

We then generalize the measure of the integral to $D = 4 - \delta$ dimensions and, after performing a Wick rotation to recover the Euclidean signature, we use the following result (See Appendix B of [194] for more details)

$$\int \frac{d^Dk}{(2\pi)^D} \frac{(k^2)^a}{(k^2 - \Delta)^b} = i(-1)^{a-b} \frac{1}{(4\pi)^{D/2}} \frac{1}{\Delta^{b-a-\frac{D}{2}}} \frac{\Gamma\left(a + \frac{D}{2}\right)\Gamma\left(b - a - \frac{D}{2}\right)}{\Gamma(b)\Gamma\left(\frac{D}{2}\right)} \tag{1.31}$$

to obtain

$$\begin{aligned}\Pi^{\mu\nu}_{\rm QED} &= -8p^2\eta^{\mu\nu} \lim_{D\to 4} \frac{e^2\mu^{4-D}}{(4\pi)^{D/2}} \Gamma\left(2 - \frac{D}{2}\right) \int_0^1 dx x(1 - x) \left(\frac{1}{m^2 - p^2x(1 - x)}\right)^{2-\frac{D}{2}} \\ &= -\frac{e^2}{2\pi^2} p^2\eta^{\mu\nu} \lim_{\delta\to 0} \int_0^1 dx\, x(1 - x) \left[\frac{2}{\delta} + \ln\left(\frac{\tilde{\mu}^2}{m^2 - p^2x(1 - x)}\right) + \mathcal{O}(\delta)\right].\end{aligned} \tag{1.32}$$

In Eq 1.32 we we use $k^\mu k^\nu \to \frac{1}{D}\eta^{\mu\nu}k^2$ in D dimensions, to rewrite the $k^\mu k^\nu$ term and we define $\tilde{\mu}^2 = 4\pi\mu^2 e^{-\gamma_E}$ where γ_E is the Euler-Mascheroni constant.
In conclusion, we can rewrite Eq. 1.28 as

$$i\Pi^{\mu\nu}_{\rm QED} = ie^2 \left(-p^2 g^{\mu\nu} + p^\mu p^\nu\right) \Pi_{\rm QED}\left(p^2\right), \tag{1.33}$$

where

$$\Pi_{\rm QED}\left(p^2\right) = \frac{1}{2\pi^2} \lim_{\delta\to 0} \int_0^1 dx\, x(1 - x) \left[\frac{2}{\delta} + \ln\left(\frac{\tilde{\mu}^2}{m^2 - p^2x(1 - x)}\right)\right]. \tag{1.34}$$

[9] Just for this section we define $p^2 = p^\alpha p_\alpha$

Considering the $p^2 \to 0$ limit, for which the integral over x is straightforward to compute, $\Pi_{\rm QED}\left(p^2\right)$ results

$$\Pi_{\rm QED}\left(0\right) = \frac{1}{12\pi^2}\lim_{\delta\to 0}\left[\frac{2}{\delta} + \ln\left(\frac{\tilde{\mu}^2}{m^2}\right)\right] \tag{1.35}$$

and we obtain, as expected, that the divergence now appears as a pole in δ and depends on an energy scale μ, introduced to have a dimensionless argument of the logarithm.

2) Renormalize the divergence by reabsorbing it in the coupling constants

The second step consists in defining the renormalized coupling constants in such a way that the divergences are reabsorbed.

We consider again the Lagrangian of QED

$$\mathcal{L}_{\rm QED} = \frac{1}{4}F_{b,\mu\nu}F_b^{\mu\nu} + i\bar{\psi}_b(\partial\!\!\!/ + ie_b A\!\!\!/_b)\psi_b - m_b\bar{\psi}_b\psi_b, \tag{1.36}$$

where now we make explicit the appearance of bare quantities with the subscript b. To absorb the divergence arising in computing the loop in Fig. 1.4, we have to define the renormalized electric charge as

$$e_{\rm R}^2 := e_b^2 - e_b^4\Pi_{\rm QED}\left(p_0^2\right), \tag{1.37}$$

where p_0 is a reference scale[10], so that, solving for the bare electric charge e_b, we find

$$e_b^2 = e_{\rm R}^2 + e_{\rm R}^4\Pi_{\rm QED}\left(p_0^2\right). \tag{1.38}$$

As a result, the bare electric charge appearing in the Lagrangian is now divergent but this is not a problem as it is not the observed charge. More importantly, such divergence cancels the divergence appearing once we include the quantum correction in Fig. 1.4.
In conclusion, the Lagrangian of QED is given by the sum of the renormalized Lagrangian $\mathcal{L}_{\rm QED}^{\rm R}$ and the counterterms $\mathcal{L}_{\rm QED}^{\rm CT}$

$$\mathcal{L}_{\rm QED} = \mathcal{L}_{\rm QED}^{\rm R} + \mathcal{L}_{\rm QED}^{\rm CT}, \tag{1.39}$$

where the counterterms are defined in such a way that they cancel the divergences arising in adding the contribution of quantum corrections.

3) Fix the finite leftover with experiments (renormalization conditions)

The last step consists in imposing the renormalization conditions. In order to obtain a predictive theory, one has to fix the finite renormalized results with the

[10] Differences in the choice of p_0 result in differences in the finite leftover that has to be fixed by imposing renormalization conditions.

outcome of independent observations.

In the case under analysis, the finite part of $\Pi_{\text{QED}}\left(p^2\right)$ depends on the regularization method adopted in order to regularize the divergence. As a consequence, it has to be fixed by imposing a renormalization condition. If we were to repeat the computation using the Feynman rules derived from the Lagrangian in Eq. 1.39, we would have to compute the graphs represented in Fig. 1.5, where we add the contribution of $\mathcal{L}^{\text{CT}}_{\text{QED}}$ to the loop.

Figure 1.5: Renormalized self energy of photon

Feynman diagrams representing, from left to right, the counterterm and the vacuum polarization. The sum is finite as the counterterm cancels the divergences arising in the loop diagram.

As expected, we obtain that the contribution of the counterterm reabsorbs the divergence of the loop integral and $i\Pi^{\mu\nu}_{\text{QED,fin}}$ results

$$\begin{aligned} i\Pi^{\mu\nu}_{\text{QED,fin}} &= ie_R^2\left(-p^2 g^{\mu\nu} + p^\mu p^\nu\right)\left[\Pi_{\text{QED}}\left(p^2\right) - \Pi_{\text{QED}}\left(p_0^2\right)\right] \\ &= \frac{ie_R^2}{2\pi^2}\left(-p^2 g^{\mu\nu} + p^\mu p^\nu\right)\lim_{\delta\to 0}\int_0^1 dx\, x(1-x)\left[\ln\left(\frac{m^2 - p_0^2 x(1-x)}{m^2 - p^2 x(1-x)}\right)\right], \end{aligned} \tag{1.40}$$

where in the second line we use the result in Eq. 1.34. Even if the second line of Eq. 1.40 is finite and we can safely take the limit $\delta \to 0$, it is not uniquely defined. In conclusion, a renormalization condition has to be imposed in order to get rid of this scheme-dependence.

1.2.3 Infinite vacuum energy?

Let's consider the action for a massless scalar field $\hat{\phi}$ in Minkowski space

$$S_\phi = \int d^4x\, \partial_\mu\hat{\phi}\partial^\mu\hat{\phi} \tag{1.41}$$

and write the field in terms of the mode function u_k and creation and annihilation operators $\hat{a}_k$ and $\hat{a}_k^\dagger$

$$\hat{\phi}(x) = \int \frac{d^3k}{(2\pi)^3}\left[\hat{a}_{\vec{k}} u_k + \hat{a}^\dagger_{\vec{k}} u_k^*\right], \tag{1.42}$$

where the operators $\hat{a}$ and $\hat{a}^\dagger$ obey the commutation relations

$$\begin{aligned} \left[\hat{a}_{\vec{k}}, \hat{a}^\dagger_{\vec{k}'}\right] &= (2\pi)^3\delta^3(\vec{k} - \vec{k}'), \\ \left[\hat{a}_{\vec{k}}, \hat{a}_{\vec{k}'}\right] &= 0, \\ \left[\hat{a}^\dagger_{\vec{k}}, \hat{a}^\dagger_{\vec{k}'}\right] &= 0. \end{aligned} \tag{1.43}$$

By considering the stress energy tensor derived from the action in Eq. 1.41

$$\hat{T}^{\phi}_{\mu\nu} = \partial_\mu\hat{\phi}\partial_\nu\hat{\phi} - \frac{1}{2}\eta_{\mu\nu}\partial_\alpha\hat{\phi}\partial^\alpha\hat{\phi} \tag{1.44}$$

the results for the vacuum energy is divergent[11]:

$$\rho := -\langle 0|\hat{T}^{\phi}{}_0{}^0|0\rangle = \int \frac{d^3k}{(2\pi)^3}\,\frac{w_k}{2} \sim k^4 \sim \infty, \tag{1.45}$$

where we assume that solving the equation of motion (EOM), the mode function results $u_k = \frac{e^{-ik_\mu x^\mu}}{\sqrt{2w_k}}$ and we define $k^\mu = (w_k, k)$, $w_k = |k^2|$. In Minkowski space the divergence is simply discarded, for example by the use of normal ordering. This can be done because in flat spacetime just the difference of energies has a physical meaning, and the energy of the vacuum can be simply rescaled to zero. In curved spacetime this procedure is more subtle as, simply put, being energy the source of gravity, one has to be careful in reabsorbing the energy of the vacuum (See section 6.1 of [48] for more details). As a consequence, such divergence cannot be simply thrown away and we are not free to rescale the zero point of energy. Instead, the renormalization procedure allows to make sense to such divergence by reabsorbing it via the redefinition of the action of the background metric.
In order to better understand the difference between Minkowski and curved spacetimes, we repeat the computation of the energy of a massless scalar field considering now a spatially flat FLRW background described by the scale factor ([48])

$$a(t) = \sqrt{1 - A^2t^2}, \tag{1.46}$$

where A is a constant. In four dimensions the mode function in conformal time results

$$u_k = \frac{1}{a(t)}\frac{1}{\sqrt{2}(k^2 + A^2)^{\frac{1}{4}}}e^{-ik\cdot x + i\sqrt{k^2+A^2}\tau} \tag{1.47}$$

from which we can recover the result in Minkowski in the limit $a(t) = 1$, $A = 0$. The energy density results (we recall that H is the Hubble parameter)

$$\rho = -\langle 0|T^{\phi}{}_0{}^0|0\rangle = \frac{1}{32\pi^3 a(t)^4}\int d^3k\,\left[\sqrt{k^2 + A^2} + \frac{k^2 + H^2}{\sqrt{k^2 + A^2}}\right] \tag{1.48}$$

which is, as expected, UV-divergent. by introducing the UV-cutoff $e^{\epsilon\sqrt{k^2+A^2}}$ and expanding the integral in powers of ϵ, we obtain the regularized result

$$\rho = \frac{1}{32\pi^2 a(t)^4}\lim_{\epsilon\to 0}\left[\frac{48}{\epsilon^4} + \frac{4H^2 - 8A^2}{\epsilon^2} + A^2(2H^2 - A^2)\log\epsilon\right] + \mathcal{O}(\epsilon^0). \tag{1.49}$$

From the result in Eq. (1.49) we not only recover the Minkowski-like quartic divergence, but also divergences that depend on the scale factor. We indeed obtain that

[11] In what follows we drop the vector notation and with k we refer to the spatial components.

the quadratic and log divergence in Eq. (1.49) redshift and, even if we discard the zero-point divergence that we would obtain in Minkowski space, the energy density is still divergent in the limit $\epsilon \to 0$. As a consequence, the usual normal ordering prescription is not enough to get rid of the vacuum energy divergences in curved spacetime and one has to refer to the renormalization procedure to obtain a finite result.
As we will see in detail in this thesis, to obtain a finite answer one has to follow the procedure reviewed in Section 1.2.2 to reabsorb the divergences by redefining the bare constants of the background action.

1.3 Work in this thesis

This thesis is divided in two parts, in each of which the goal is to tackle the renormalization of divergences arising in including quantum vacuum tensor pertutbations on a curved spacetime. In the first part we adopt a foliation specific description as we aim to study divergent quantities on backgrounds of cosmological interest. In the second part, in which we work in a fully covariant formalism, we retrace and expand the results of the first part.

Part I: Foliation specific formulation

- **Chapter 2:** we provide the details of vacuum GWs constraints from N_{eff} bounds and motivate the work in this thesis. We review how primordial vacuum tensor fluctuations are included in estimating N_{eff} by examining the derivation of the stress energy tensor for GWs first derived by Isaacson in ([123]). We motivate on why it is appealing to include vacuum GWs in the radiation-like content of the universe by reminding the role of BBN in constraining N_{eff}. To conclude, we highlight the caveats that motivated our work, such as the appearance of an UV regulator in what should be a physical result and the regime of validity of energy density of GWs, namely sufficiently high frequency signals for which the curvature of the background can be neglected.

- **Chapter 3:** considering that many cosmological observables derive from primordial vacuum fluctuations evolved to late times, we present the process of renormalization by studying a massless spectator scalar field on a FLRW background. This apparently simple working example brings to light many relevant results. We first demonstrate that infinities arise in observables that represent statistical draws from some underlying quantum field theoretic framework. We then elaborate on how infinities can be regularized: we show that in spite of the ubiquity of scaleless integrals, UV divergences can still be meaningfully extracted using dimensional regularization and that the coefficients of the logarithm divergence do not depend on the regularization method. We both analyze the divergences arising in computing the two point function in different backgrounds and in computing the components of the stress energy

tensor. In studying the latter, we conclude that regularization methods which preserve general covariance are to be preferred. By studying backgrounds that transition from finite duration inflation to radiation domination, we show that UV and IR scales corresponding to the beginning and end of inflation do not appear as UV cutoffs and motivate that observables cannot depend on the latter, although will certainly depend on the former. Furthermore, it appears that IR divergences are an artifact of the dS limit and are cured for finite duration inflation.

- **Chapter 4:** we address the caveats highlighted in Chapter 2. By undoing the steps that relied on a high frequency signal for which the effect of curvature can be neglected, we derive an improved stress tensor that does not presume a prior scale separation. To understand whether one can meaningfully constrain vacuum GWs from $N_{\rm eff}$ bounds, we specify the improved formula of the energy density on backgrounds that transition from finite duration inflation to radiation domination. We then comment on the physical interpretation of the power spectral density of vacuum GWs on a FLRW background, and we find that the regularized energy density is consistent with the results of the scalar case studied in Chapter 3 (scheme independence of UV logarithmic divergences and need of using schemes that preserve general covariance to obtain counterterms constructed from geometric invariants). After the subtraction of the divergences arising in the regularized energy density, renormalization conditions must be imposed by measurements at some scale, mindful of scheme and background dependence. We review this process considering first the energy density of a scalar field derived in Chapter 3, and then the improved energy density of vacuum GWs, obtaining a final result that does not depend on UV regulators. We conclude by highlighting the inextricable connection between inferring $N_{\rm eff}$ bounds from vacuum tensor perturbations and the process of background renormalization.

  Chapters 3 and 4 are based on [169]:
  An Étude on the Regularization and Renormalization of Divergences in Primordial Observables
  A. Negro and S. P. Patil, *Riv.Nuovo Cim.* 47 (2024) 3, 179-228.

Part II: Covariant formulation

- **Chapter 5:** we review the formalism needed to study vacuum GWs as a massless spin-2 particle on curved spacetime. Considering that we aim to address the caveats reviewed in Chapter 2 in a fully covariant formulation, we introduce the fundamental concepts of QFT in curved spacetime to define the renormalized stress energy tensor for GWs as the variation of the effective action with respect to the background metric. After reviewing the background

field method to obtain the 1-loop effective action, we remind the Faddeev-Popov procedure to fix the gauge at the level of the action. Lastly, we derive the Lagrangian formulation of a radiation-like fluid in the context of $P(X)$ theories.

- **Chapter 6:** the derivation, regularization and renormalization of the graviton stress tensor is addressed in a fully covariant formalism. We obtain the regularized graviton action by gauge-fixing via the Faddeev-Popov procedure and adopting Hadamard regularization techniques to isolate UV divergences. After defining the counterterms at the level of the action, from which the renormalized stress tensor can be derived by variating with respect to the backgorund metric, we comment on the finite contributions which are absorbed in the process of imposing renormalization conditions. We then proceed to specify our otherwise general results in a RD universe, to reexamine and connect with the results of Chapter 4. We discuss the imposition of renormalization conditions via a physical measurement at some fixed scale, which we retrace for primordial GWs sourced from vacuum fluctuations through direct or indirect observation. In agreement with our conclusions of Chapter 4, we obtain that one cannot constrain vacuum tensor perturbations from N_{eff} bounds: the net effect of including vacuum tensor perturbations is to shift the normalization of otherwise unobservable bare quantities. In addition, from the covariant description we find divergences that require higher order corrections to the Einstein Hilbert action to be reabsorbed and that the regularized stress tensor associated with the shifted radiation-like content is no longer traceless, features that were not evident in the foliation dependent description.

Chapter 6 is based on [170]:
Hadamard Regularization of the Graviton Stress Tensor
A. Negro and S. P. Patil, arXiv:2403.16806, (2024).